Na$^+$ Charge Tuning through Encapsulation of Sulfur Chromophores in Zeolite A and the Consequences in Adsorbent Properties

Sandra Loera,[*,†] **Philip L. Llewellyn,**[‡] **and Enrique Lima**[†]

Instituto de Investigaciones en Materiales, UNAM, Circuito Exterior. A. P. 70-360, 04510 México, D. F. Mexico, and Laboratoire Chimie Provence (UMR 6264), CNRS-Universités Aix-Marseille I, II & III, Centre de St Jérôme, 13397 Marseille cedex 20, France

Received: December 11, 2009; Revised Manuscript Received: March 16, 2010

The effect of sulfur chromophores on the Na$^+$ cation charge was investigated. Carbon dioxide and methane adsorption into zeolite A were modified by the encapsulation of the chromophores due to the interaction between Na$^+$ and S$_x^-$ ($x = 2$ or 3). Indeed, the isotherms and enthalpies of CO$_2$ and CH$_4$ depended on the amount of trapped sulfur as well as on the zeolite structure. In this work, we also propose the mechanism of polysulfide formation and structural transformation when the molar ratio S/Na$_2$CO$_3$ = 0.3 and the mechanism of reaction between sulfur and sodium carbonate and diffusion into the LTA (Linde Type A) structure when S/Na$_2$CO$_3$ = 5.0.

1. Introduction

Zeolites are porous crystalline aluminosilicates with regular cavities of molecular dimensions connected through windows.[1] These materials can be classified according to features, such as Si/Al ratio or structural properties.[2] Some zeolites have a high Si/Al ratio (sodalite, zeolite Y, mordenite, silicalite, among others), whereas another group of zeolites has a low Si/Al ratio which can equal 1, such as zeolite A. The aluminum in the zeolites has to be tetracoordinated, and thus, a charge deficiency is present in the framework which is balanced with exchangeable cations such as Na$^+$. Zeolite A has the lowest Si/Al ratio, that is, the highest exchange capacity.

The Na A zeolite network is constituted by three cavities whose diameter dimensions are 11.4, 6.6, and 2.2 Å (Figure 1). Sodium cations are located in well-known sites,[1] and they determine the electric field gradient inside these cavities as well as on the connecting windows.

If cations are exchanged, the local charge varies only discretely and it is hard to tune it. However, some interesting studies have been reported on anion occlusion into the zeolite structure. Ag^{2+} containing zeolites have been used to retain I^{-}.[3,4] Indeed, silver is able to replace sodium and then interact locally with iodine. Although other anions such as sulfur have been confined into zeolites, the charge modifications have not been completely discussed.

Sulfur forms the chromophore anions S$_2^-$ (yellow), S$_3^-$ (blue) and S$_4^-$ (red) whose optical properties are well-known.[5] In this sense, many studies have concentrated on the sulfur incorporation procedure. Thermal treatment of a mixture of sulfur, sodium carbonate, and zeolite A was used in most syntheses. In 1994, Choi et al.[6] followed the reaction between sodium carbonate and sulfur; they proposed a mechanism for polysulfide formation.

The reaction between sulfur and sodium carbonate occurs from about 260 °C via a disproportionation reaction giving a reduced (Na$_2$S$_4$) and an oxidized form (Na$_2$S$_2$O$_3$). When sodium
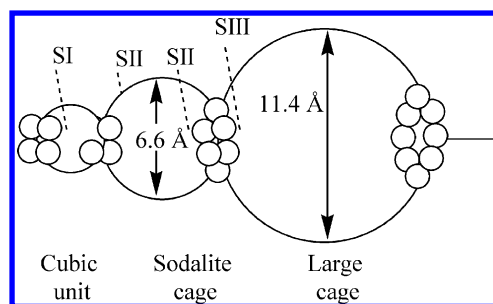

Figure 1. Window size of zeolite A cavities.

carbonate is in excess (S/Na$_2$CO$_3$ < 3.3), S$_4^{2-}$ is the only polysulfide formed; However, when sulfur is in excess, the reduced polysulfide S$_5^{2-}$ is preferred. Moreover, the theoretical maximum insertion of the chromophores is one S$_x^-$ per sodalite cavity with $x = 2$ or 3.[7,8] Recently, green materials constituted by polysulfides and zeolite have been shown to present a LTA (Linde Type A) structure, whereas the blue samples have a sodalite structure. The ratio S$_2^-$/S$_3^-$ of the green samples is higher than the ratio S$_2^-$/S$_3^-$ of the blue samples.[9,10]

The present work aims to modify the lattice positive charge of zeolite A through the encapsulation of sulfur anions. The samples were prepared at low temperature to preserve the zeolite structure.[10] The zeolite cation charge can be inferred through adsorption enthalpy of carbon dioxide when compared to methane used as probe molecules.

2. Experimental Section

2.1. Materials. Zeolite Na A, type 4A, was provided by Union Carbide. Anhydrous sodium carbonate (purity ≥ 99.0%) and sulfur (purity = 99.999%) were from Aldrich. Carbon dioxide and methane, both with purity of 99.995%, were supplied by Air Liquide (Alphagaz, France).

2.2. Synthesis. The samples were prepared by thermal treatment of zeolites, sulfur, and sodium carbonate ground together, as in our previous work.[10] The molar ratios S/Na$_2$CO$_3$ were 0.3 and 5.0 for samples labeled as ZAS0.3 and ZAS5.0 respectively. The sulfur content was 0.2 g of sulfur per gram

* To whom correspondence should be addressed. Telephone: (+5255) 53189570. E-mail: sls@correo.azc.uam.mx.
† Instituto de Investigaciones en Materiales, UNAM.
‡ CNRS-Universités Aix-Marseille I, II & III.

of zeolite. The reagents A zeolite, Na_2CO_3, and S were outgassed under vacuum (10^{-4} Torr) at 150, 200, and 25 °C, respectively. Then the mixture was sealed under vacuum (10^{-4} Torr), heated gradually up to 365 °C, and maintained at this temperature for 12 h before being quenched before opening the capsules. To remove residual traces of Na_2CO_3, the obtained solid was washed with deionized water and finally dried at room temperature under air.

2.3. Characterization. *2.3.1. Energy Dispersive X-ray (EDX) Spectroscopy.* Energy dispersive X-ray spectroscopy was performed with an EDS instrument, EDAX DX4 SUTW-USA, coupled to a Cambridge S90B scanning electron microscope, Great Britain system. It has to be emphasized that the samples were not covered with a Au-sputtered film. In this way, eventual impurities as well as the Si/Al ratio of the materials were measured with a high precision. This instrument is able to detect semiquantitatively elements whose atomic number is higher than that of boron. The beam was focused in order to cover an area of 6 μm^2 and a depth of 4 μm.

2.3.2. X-ray Powder Diffraction (XRD). A Siemens D500 powder diffractometer coupled to a copper anode X-ray tube was used to identify the compounds present in each sample. The filtered Kα radiation was selected with a diffracted beam monochromator. The powdered samples were mounted on a platinum sample holder whose (111) Pt peak was used as a standard to correct the (311) peak shift of the zeolite A cubic structure and the (410) and (002) peaks for the hexagonal structure.

2.3.3. Fourier Transform Infrared (FTIR) Spectroscopy. The FTIR spectra (500−4000 cm^{-1}) were obtained with a resolution of 2 cm^{-1} at room temperature on a Perkin-Elmer 1600 series FTIR spectrometer, fitted with a DTGS detector. The samples were previously prepared as KBr pellets.

2.3.4. Ultraviolet−Visible (UV−vis) Spectroscopy. The UV−vis spectra were recorded on a Cary 300, Varian spectrometer using diffuse reflectance mode in the range 250−800 nm. The powdered samples were mixed with MgO in order to reduce the intensity of the signal (1 g of sample per 1 g of MgO).

2.3.5. Scanning Electron Microscopy (SEM). The morphology and particle size of the samples were acquired by using a scanning electron microscope Philips XLS 30 ESEM, The Netherlands, with a field emission cathode. The samples were previously covered with gold to avoid charge problems. The particle size distributions were obtained by measuring ca. 300 particles in the SEM micrographs.

2.3.6. Thermogravimetric Analysis (TGA). The experiments were preformed under air atmosphere at a rate of 5 °C/min with a TA TGA Q500 apparatus (TA Instruments, USA). The samples were heated from room temperature to 900 °C. TGA provided the maximum water content and the thermal stability of each sample.

2.3.7. Adsorption Microcalorimetry. The adsorption of CO_2 and CH_4 was carried out at 303 K. Prior to the adsorption experiment, the samples were outgassed under a vacuum of 10^{-3} mbar at 473 K for about 12 h.[11] Each experiment was repeated several times in order to corroborate the reproducibility.

3. Results

3.1. Surface Elemental Composition. To check that sulfur diffused into the zeolite, EDX analyses, which are surface analyses, were preformed. The quantitative compositions obtained by EDX spectroscopy of ZA, ZAS0.3 and ZAS5.0 are shown in Table 1. More sulfur is found on the surface of ZAS5.0 than on the ZAS0.3 sample. Note that synthesis of both samples

TABLE 1: Chemical Composition (atom %) by EDX of Zeolite A and Sulfur Treated Samples

element	ZA	ZAS0.3	ZAS5.0
O	61.67	49.73	55.86
Na	12.95	16.73	14.05
Al	12.54	13.36	11.86
Si	12.83	14.74	12.13
S	0	5.45	6.10

started with same sulfur amount but with different sodium carbonate.[10] Sodium carbonate/sulfur ratio determines the nature of sulfides species, which behave differently on zeolite framework. Then, nominal sulfur content differs for ZAS samples. The molar ratio Si/Al is 1.02 for ZAS5.0 which is within the error range of the Si/Al ratio of zeolite A but 1.10 for ZAS0.3.

3.2. Crystalline Compounds. The X-ray diffraction patterns of the ZA, ZAS0.3, and ZAS5.0 samples are compared in Figure 2. The (a) pattern corresponds to fully crystalline zeolite A whose cell parameter is 12.28 Å. In sample ZAS0.3 (Figure 2b), with less nominal sulfur content, the zeolite peaks are less prominent, and a hexagonal $Na_8(Al_6Si_6O_{24})S$ ($a_0 = b_0 = 5.22$ Å and $c_0 = 12.74$ Å) compound is identified with traces of Na_2SO_4 labeled as (●). Sample ZAS5.0, with the highest sulfur content (Figure 2c), corresponds to a mixture of crystalline phases: mainly a cubic one, $Na_{11}Al_{11}Si_{13}O_{48}S_{16}$ ($a_0 = 12.19$ Å), and a very small amount of an orthorhombic one ($NaAlS_3$, labeled as ◆). The differences between ZA and the cubic phase found in ZAS5.0 are the relative peak intensities and the presence of some extra peaks (211), (310), (222), (400), and (432).

In summary, the ZAS5.0 sample can be considered as constituted by sulfur containing LTA and the ZAS0.3 sample would seem to be essentially a newly sulfur containing material with a cancrinite structure. In both samples, the sulfur was incorporated into the formed compounds.

3.3. Polysulfide Species (FTIR and UV−vis). The FTIR spectrum of the ZA sample (Figure 3a) shows the well described features for an aluminosilicate framework.[12] In the (b) spectrum, obtained with ZAS0.3, only a small band at 3500 cm^{-1} corresponding to stretching vibration of OH$^-$ groups is observed. Indeed, when water molecules are present, the absorption bands in the 3200−3700 cm^{-1} window are observed.[13] The lack of this band in (b) is in contrast with the other two spectra in which
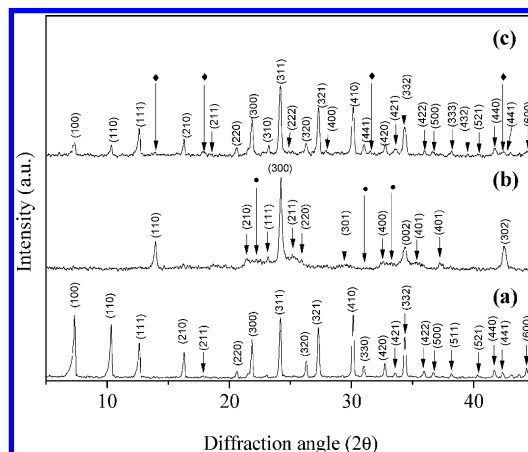

Figure 2. X-ray diffraction patterns: (a) ZA, (b) ZAS0.3, and (c) ZAS5.0. Numbers above peaks correspond to Miller indexes determined with the JCPDS cards: 4-0298 for (a), 38-0515 for (b), and 71-0898 for (c). Peaks labeled (◆) and (●) correspond to $NaAlS_3$ (41-0938 JCPDS card) and Na_2SO_4 (25-0111 JCPDS card), respectively.

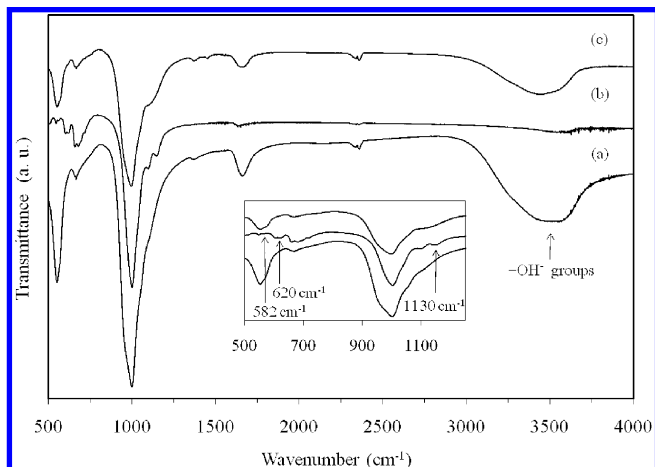**7882** *J. Phys. Chem. C, Vol. 114, No. 17, 2010*

Loera et al.

Figure 3. FTIR spectra: (a) ZA, (b) ZAS0.3, and (c) ZAS5.0.
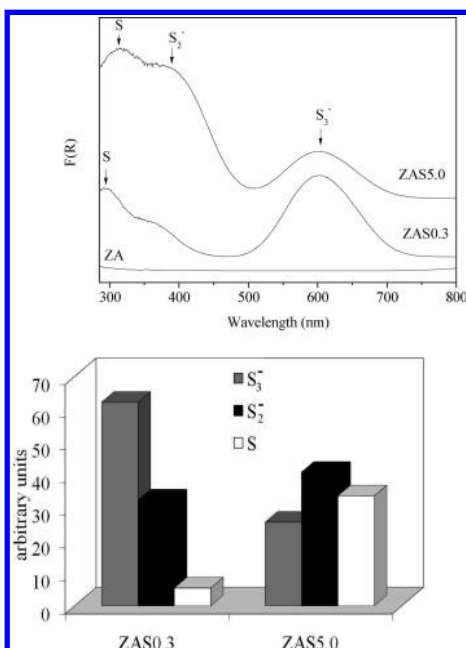

Figure 4. (a) UV−vis spectra of ZA, ZAS0.3, and ZAS5.0. (b) Comparison of the relative amounts of chromophore (S_3^-, blue and S_2^-, yellow) and elemental sulfur (yellow).

Figure 5. (right) SEM images of ZA, ZAS0.3, and ZAS5.0 samples and (left) corresponding particle size distributions.

a broad and intense band appears in that region. Thus, while many zeolites contain large amounts of water, it can be noted that the $Na_8(Al_6Si_6O_{24})S$ compound is a nonhydrated ceramic.[14]

A doublet and a single band at 620 cm^{-1} appear in the (b) spectrum which may be attributed to S_2^-.[15] A difference between the (a) and (c) spectra is that the (c) spectrum, with ZAS5.0, shows weak bands at 582 and 1130 cm^{-1}, assigned to vibration of S_3^- and sulfate groups, respectively.

The UV−vis spectrum of ZA was used as reference due to the white color and that it does not present absorption in the studied spectral window (Figure 4a). The UV−vis spectra of the sulfur containing materials show three main bands which indicate the presence of S_2^- ($\lambda = 390-400$ nm) and S_3^- ($\lambda = 600-610$ nm) chromophores and of elemental sulfur ($\lambda = 300-350$ nm). The band at 600 nm is more intense in the spectrum of ZAS0.3 than in that of ZAS5.0, while the band at 400 nm is enhanced in the ZAS5.0 spectrum. A high percentage of S_3^- leads to blue samples; and the mixture of S_2^-, S_3^-, and S generates yellow or green samples. The color points toward the sulfur chromophore insertion inside the cavities of the resulting materials, blue for ZAS0.3 and green for ZAS5.0.
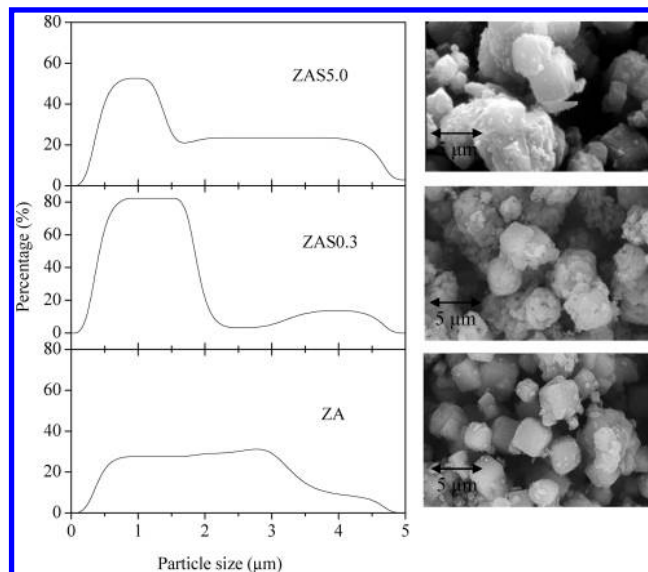
To present more graphically the variation in the relative amounts of S_2^-, S_3^-, and S, the UV−vis peaks were deconvoluted and the corresponding area estimated. Then, values were normalized to the number of sulfur atoms in each chomophore[16] and presented as a histogram (Figure 4b). Note that the amount of elemental sulfur (S) in ZAS5.0 is much higher than that in ZAS0.3, showing that when the ratio S/Na_2CO_3 is increased, the nonreacting sulfur increases not linearly. Although both chromophores (S_2^- and S_3^-) are present in both samples, it is the ratio which determines the color.

3.4. Morphology. In Figure 5, SEM images of ZA, ZAS0.3, and ZAS5.0 are shown. As expected, all samples have a cubic morphology. Particle size distributions are also presented. In both ZAS0.3 and ZAS5.0, when the zeolite was treated with sulfur, particles (ca. 1 μm) were formed on top of larger ones (ca. 4 μm).

Comparing the micrographs, the cubic shape of zeolite A particles (sample ZA) is modified in the sulfur containing materials (ZAS0.3 and ZAS5.0). In ZAS0.3, the cubic particles are more covered by small entities whose shape is irregular. The sample ZAS5.0 morphology is intermediate. Therefore, better covering of large zeolite particles by smaller ones was observed at higher initial amount of Na_2CO_3. It seems as if the cubic zeolite particles were divided. Particle size distributions agree with the previous qualitative remarks. The ZA particle size distribution is broad from $D = 0.5$ to $D = 3.0$ μm, and no maximum is observed. However, the ZAS0.3 and ZAS5.0 samples present a clear maximum at $D = 1$ μm corresponding to the irregular particles. In ZAS0.3, the proportion of particles smaller than 2 μm is much higher than that in ZAS5.0.

3.5. Thermal Behavior. Thermogravimetric curves of ZA, ZAS0.3, and ZAS5.0 samples are shown in Figure 6. The total weight loss in ZA and ZAS5.0 was 20%, whereas ZAS0.3 lost only 10%; this total weight loss can be attributed to water and sulfur sublimation (96 °C).

The loss observed with ZA (15 wt %) at temperatures below 200 °C (Figure 6 (ZA)) is probably due to the elimination of water molecules located in the large cavity or to the elimination of molecules which do not occupy definite lattice sites. At temperatures higher than 400 °C, 5 wt % was lost, due to the loss of the intracrystalline water.[1]

The TGA curve of ZAS0.3 does not present weight losses at 200 °C as occurred in ZA or ZAS5.0, but with differential
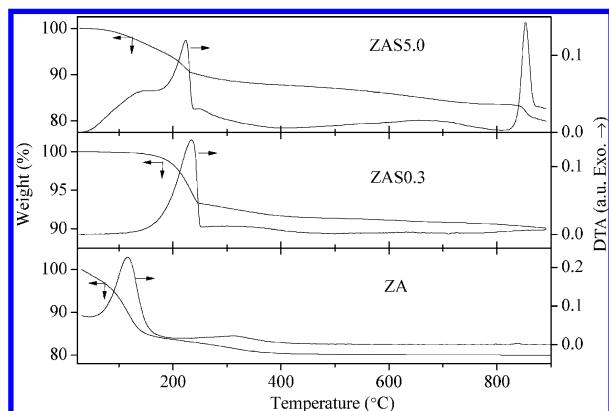
Figure 6. Comparison of the thermogravimetric curves of zeolite A and sulfur containing samples, under air flux.

thermal analysis (DTA) a peak at 250 °C is observed, due to the sulfur removal as in ZAS5.0. The sample ZAS0.3 did not lose polysulfide even at 900 °C. This result is in good agreement with FTIR spectroscopy, and indeed sample ZAS0.3 is not hydrated.

The first weight loss of ZAS5.0 was at temperatures below 200 °C; it may correspond to water loss as in the ZA sample. The following peak, on DTA at 250 °C, can correspond to sulfur elimination as SO$_2$ or H$_2$S (Figure 6, ZAS5.0).[6] The last peak (ca. 900 °C) is identified as a polysulfide loss in accordance with a mass spectrometer experiment, the spectrum is shown in the Supporting Information.

3.6. Gas Adsorption. The gas adsorption microcalorimetry has been used to probe both any porosity of the samples as well as any surface chemistry. Indeed, methane is a molecule with no permanent electrical moment and can be used to probe the textural properties of the samples, whereas carbon dioxide, with a quadrupole moment, can be used to further probe any variations regarding surface chemistry.

From TGA data, we determined the temperature of dehydration of the samples used prior to the microcalorimetry experiments. Thus, samples were treated at 200 °C under a vacuum of less than 10^{-3} mbar for 16 h prior to adsorption. Figure 7 shows the adsorption uptake and the adsorption enthalpy obtained with carbon dioxide or methane. The CH$_4$ adsorption isotherm is type-III for ZAS0.3 and ZAS5.0 which suggests a weak interaction between adsorbate and adsorbent. However, the isotherm turns out to be type-I for ZA/CH$_4$. The CH$_4$ adsorbed at 20 bar was 0.52 mmol/g of ZAS0.3 and 0.46 mmol/g of ZAS5.0. The CH$_4$ adsorption curve of ZA did not reach a plateau up to 25.0 bar. Methane molecules can reach the free space of ZA zeolite cavities and interact with Na$^+$ cations.

The adsorption isotherm obtained with carbon dioxide is of type-I shape which suggests micropore filling.[17] The isotherms obtained with the sulfur containing samples are linear with a much lower uptake. Indeed, the maximum adsorbed amount is 4.5 mmol of CO$_2$/g of ZA; at 20 bar, it is 0.4 mmol of CO$_2$/g of ZAS0.3 and 1.2 mmol of CO$_2$/g of ZAS5.0. Note that the amount adsorbed in ZAS0.3 is 10 times less than that in ZA and 3 times less than that in ZAS5.0. Gas molecules can interact straightforwardly with Na$^+$ cations of ZA, as these are quite accessible. Instead, in ZAS5.0, the polysulfides must be occluded into the sodalite cavities as suggested by Gobeltz-Hautecoeur et al.[18] and, therefore, the interaction with Na$^+$ is more difficult. In the hexagonal structure of ZAS0.3, the cavities have small dimensions: 5.9 Å for the window of the large cavity and 3 Å for the windows of the cancrinite cavity. Only 8.9% of the CO$_2$ amount adsorbed in ZA can be adsorbed on this material.
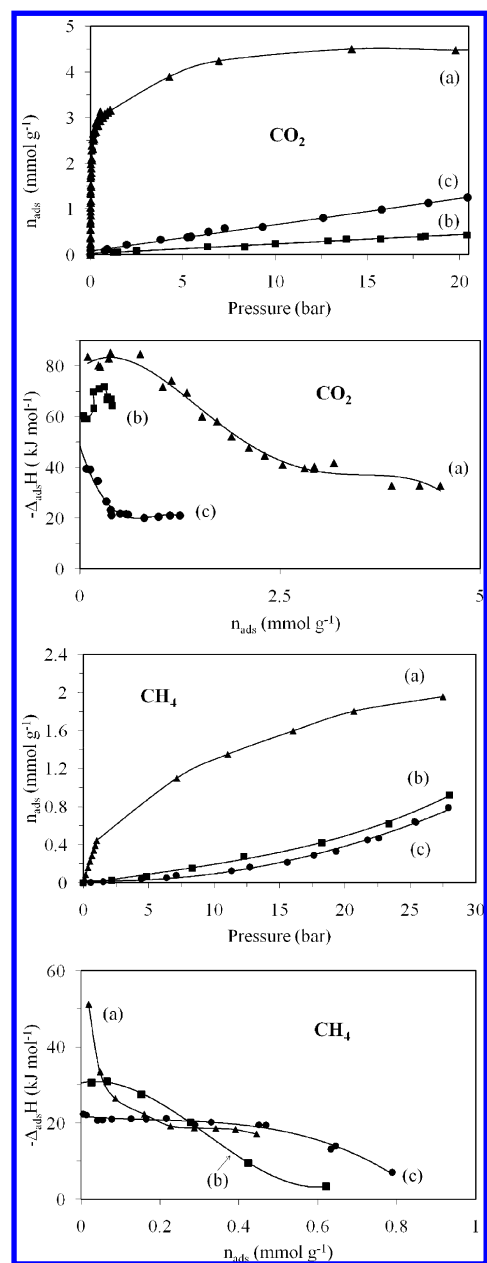

Figure 7. Isotherms and enthalpies of CO$_2$ and CH$_4$ adsorption on (a) ZA, (b) ZAS0.3, and (c) ZAS5.0 at 303 K.

The Henry constants can be estimated, being 34.11 and 0.11 mmol/g for CO$_2$/ZA and CH$_4$/ZA, respectively. As the Henry constant for CO$_2$/ZA is much larger than that for CH$_4$/ZA, CO$_2$ adsorption would seem to be much more energetic than methane which is due to the sodium.

The enthalpies of adsorption of carbon dioxide and methane on ZA (Figure 7) have a typical shape.[11] The enthalpy of adsorption of methane extrapolated to zero coverage is close to -50 kJ/mol; this value reflects the interaction of CH$_4$ with the cations Na$^+$. CO$_2$ enthalpy values are much higher than those observed for CH$_4$, and thus, the quadrupole moment of CO$_2$ interacts with the energetically homogeneous surface due to the presence of sodium cations. For instance, the extrapolated value obtained for zero coverage is close to -80 kJ/mol. The gradual decrease in enthalpy with increasing coverage in enthalpy curves, for both CH$_4$ and CO$_2$, indicates a pore filling process.

The values of enthalpy adsorption of CO$_2$ and CH$_4$ are very influenced by the composition of zeolite. Enthalpy adsorption

7884 *J. Phys. Chem. C, Vol. 114, No. 17, 2010*

Loera et al.

values of CO_2 in sulfur containing zeolites are always lower than those obtained in ZA reference zeolite. However, an atypical behavior is observed for ZAS0.3 where at low values of coverage the adsorption enthalpy is more negative and then decreases, indicating heterogeneities at the surface responsible for adsorption.

For CH_4, the values of enthalpy adsorption on sulfur containing samples trend to lower values at zero loading of adsorbate if compared with the ZA sample. Then a decrease is observed but the slopes vary significantly depending on the value of coverage. As a consequence, several common points were observed for three adsorbents. For instance, at n_{ads} close to 0.28 mmol/g in three adsorbents, the adsorption enthalpy is around 20 kJ/mol. Note, however, that for lower and higher amounts of adsorbate, the three curves are very different which indicates that the three surfaces are texturally different.

4. Discussion

4.1. Polysulfides Trapped into Aluminosilicate Structures. EDX was used to confirm the presence of sulfur in the as-prepared material as well as to estimate the local surface Si/Al molar ratio. The mass spectrometry data support (Supporting Information) that appreciably more water is lost in two steps. Besides, the formation of SO_2 (m/z 64) and SO (m/z 48) prove the polysulfides oxidation which is around 5% wt. This result suggests that the content of sulfur, as determined by EDX, is representative of the overall material. The Si/Al molar ratio 1.10 for ZAS0.3 was different from the Si/Al = 1.02 of zeolite A. Such a difference cannot be explained simply as the compound identified in XRD is hexagonal structure and has a Si/Al ratio of 1. This apparent contradiction is related to the resolution and main principles of each technique. The EDX technique is a surface analysis corresponding to an area of 6 μm^2 and a depth of 4 μm. The EDX result, then, corresponds to an Al-deficient layer of the material. Therefore, the surface of the hexagonal particles must be constituted by those zones and small amounts of detrital alumina. The assumed alumina could not be observed by X-ray diffraction. Indeed, to detect a compound by XRD, this compound has to be crystalline, it has to present a concentration higher than 3%, and the crystals have to be larger than 40 Å. The same Si/Al ratio as in ZA is obtained in ZAS5.0; in this sample, the volume and the surface composition are, then, the same, and no Al-deficient layers are observed. Such differences in Si/Al ratios can be correlated to S/Na_2CO_3; indeed, ZAS0.3 contains more Na_2CO_3 and therefore the reaction heat is much higher. Aluminum is then expected to be able to diffuse into the zeolite particle and to form occluded alumina clusters.[19]

The XRD patterns correspond to a hexagonal structure, $Na_8(Al_6Si_6O_{24})S$ and Na_2SO_4 for ZAS0.3. This structure has been reported by Hund[20] as a cancrinite type structure (CAN) containing sulfur. The corresponding cell parameters are $a_0 = b_0 = 5.19$ Å and $c_0 = 12.66$ Å. In our work, the measured cell parameters are $a_0 = b_0 = 5.20$ Å and $c_0 = 12.76$ Å. The difference in the c direction is significant (0.1 Å). This result shows that sulfur is periodically distributed in the cancrinite type lattice and that it introduces a stress in the network such that it becomes more expanded in the c direction.

Further, in sample ZAS5.0, a mixture of LTA type structure $(Na_{11}Al_{11}Si_{13}O_{48}S_{16})$ and an orthorhombic phase is obtained. The cell parameters of the LTA structure in ZAS5.0 decrease from 12.28 to 12.19 Å due to the strong interaction between sulfur and the cations into the zeolite cavities. Note that the green sample maintains the LTA structure. However, the structure of the blue sample is CAN instead of LTA.

The ZAS0.3 and ZAS5.0 samples are blue and green, respectively. Indeed, the color of the sample has been attributed to polysulfide occlusion into the aluminosilicate structure.[1] FTIR and UV−vis support the presence of S_2^-, S_3^-, and elemental sulfur. The band corresponding to $-OH^-$ groups and the bending H_2O band around 1600 cm^{-1} are not observed in the spectrum of ZAS0.3. This result may be explained assuming that the water was used as reactant during the structural change as we show below. From UV−vis spectra, we obtained the relative amount of chromophores $S_2^-/S_3^- = 0.5$ for ZAS0.3 and $S_2^-/S_3^- = 1.6$ for ZAS5.0. This ratio was 3 times more for ZAS5.0.

Our results fit with two mechanisms of polysulfide occlusion and structural transformation. When S/Na_2CO_3 is equal to 0.3 (ZAS0.3), the mechanism may be described by the following steps:
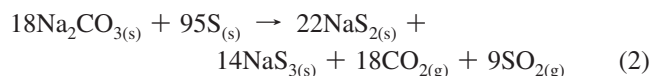
As Na_2SO_4 was observed in the XRD pattern of ZAS0.3 and S_2^-, S_3^- in the FTIR spectrum, a reaction between S and Na_2CO_3 to form polysulfides is proposed (eq 1). The reaction is a disproportionation reaction of sulfur.[8]

$$4Na_2CO_{3(s)} + 16S_{(s)} \rightarrow 3Na_2S_{5(s)} + Na_2SO_{4(s)} + 4CO_{2(g)} \tag{1}$$

$$S_5^{2-} \rightarrow S_2^- + S_3^-$$
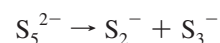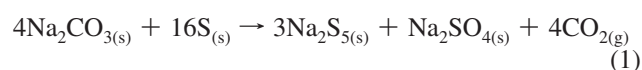
The XRD pattern of ZAS0.3 also shows that the main symmetry of the aluminosilicate is hexagonal. As it is well-known, zeolite A can transform to sodalite (cubic structure) or cancrinite (hexagonal structure) through a hydrothermal treatment at 240 °C. The heat-energy amount can be provided by the reaction between S and an excess of Na_2CO_3.[21–23] It has to be emphasized that, most probably, the hexagonal symmetry is present at a temperature lower than 365 °C as the pressure is high. In our experiment conditions, the phase transition is total to the hexagonal phase. Furthermore, the absence of water in this sample was supported by TGA and FTIR. If the EDX results are compared to those of XRD, it seems that the sulfur content in the external shell (depth 40 nm) is higher than that in the volume. Hence, the diffusion of S into the lattice is not complete.

At temperatures below 250 °C, TGA shows that the nonreacting sulfur is sublimated and the polysulfides in the cavities are present even at 900 °C. The area peak of the DTA is 6.3, and the percentage obtained by UV−vis is 5.5; these results are in agreement and show the loss of elemental sulfur not occluded into the crystalline structure. The fast cooling down has a templating effect, and the resulting material presents a high stability.

When S/Na_2CO_3 is equal to 5.0, the structure does not change and just an insertion of polysulfides into sodalite cages is observed. The amount of sulfur in excess is higher, and as no sodium carbonate remains the structure not change. The mechanism, then, can be described in three steps: First, sulfur reacts with sodium carbonate to form polysulfides. In UV−vis, S_2^- and S_3^- are the only polysulfides observed but many other polysulfides can be formed. The corresponding ratio S_2^-/S_3^- was equal to 1.6 which is in agreement with the ratio predicted by the proposed reaction (eq 2). In the FTIR spectrum, a weak band at 1130 cm^{-1}, corresponding to sulfate, is present, but no peaks of Na_2SO_4 are observed in XRD. The pressure inside the glass tube during the reaction is provided by CO_2 and SO_2.

Na$^+$ Charge Tuning

J. Phys. Chem. C, Vol. 114, No. 17, 2010 **7885**

$$18Na_2CO_{3(s)} + 95S_{(s)} \rightarrow 22NaS_{2(s)} +$$
$$14NaS_{3(s)} + 18CO_{2(g)} + 9SO_{2(g)} \quad (2)$$

The second step can be the diffusion into sodalite cages. The kinetic diameter of S_3^- has not been published yet. The kinetic diameter of the SO_2 molecule, which should be close to the diameter of the S_3^-, is equal to 3.6 Å.[7] At room temperature, the molecules cannot diffuse into the sodalite cages, due to the window size of these cages (~3.0 Å). At higher temperature (365 °C), the windows are enlarged and the molecules can diffuse due to their high kinetic energy. The breathing motion of the zeolite windows has been theoretically studied by molecular dynamics showing that the enlargement reached at $T = 1200$ °C is $\Delta D = 0.155$ Å.[24,25] DTA shows a peak at 850 °C, which has already been assigned to a polysulfide loss. At this temperature, the zeolite windows are more enlarged and polysulfides leave the structure. In a third step, chromophores are trapped into sodalite cages when temperature decreases.

4.2. Gas Adsorption. CO_2 adsorption into ZA reached a plateau at 4.5 mmol g^{-1}, and, on the other hand, enthalpy decreased until -32 kJ mol^{-1}, for amounts higher than 2.5 mmol g^{-1}. The amount of CO_2 adsorbed is in agreement with the values reported in previous works.[26–31] Hence, CO_2 molecules can reach the zeolite cavities, and they can access the large cavity but not the sodalite cages. Theoretically, it has been shown that the location of CO_2 into the zeolite lattice is in sites II and III. Furthermore, the Na$^+$–CO_2 link is through van der Waals forces due to the polarization of the CO_2 molecules. The interaction between π-electrons and cation charge is predominant. Variations of enthalpy adsorption may be interpreted in terms of material homogeneity. The values obtained at low pressure will be discussed below.

The methane isotherm of zeolite A presents the same trend as the carbon dioxide isotherm. The maximum CH_4 adsorbed was around 2 mmol g^{-1} at 27.5 bar, and the enthalpy decreased as a function of the amount adsorbed, until -18 kJ mol^{-1}. We compare our result with the ones reported.[27,28] At low pressure (<1 bar), Habgood[27] reports a maximum adsorbed amount of 2.73 mmol g^{-1}. Instead, Vermesse et al.[29] obtained negative

values without physical meaning at pressures higher than 11 bar, due to the increasing difficulty to penetrate the zeolite pores. Hence, our results contradict the values reported by Habgood and Vermesse et al. Although Habgood obtained positives values for the amount of CH_4 retained, it is 0.73 mmol g^{-1} higher than the amount reported in the present work. Habgood used lower pressure, and therefore, this contradiction has to be attributed to activation temperature (200 °C more). Indeed, the total sorption capacity appeared to be very sensitive to the degree of dehydration.[27] Vermesse et al. values are negative and as already mentioned such measurements have no physical meaning. Such differences may simply be due to pore blocking.

If CH_4 and CO_2 shape and size are compared, methane is only slightly larger than CO_2 but CO_2 presents π-electrons which are not found in CH_4. The differences in gas retention on ZA, as shown by enthalpy values, can only be attributed to the previously mentioned features, mainly the electronic properties due to the double bonds in CO_2. Indeed, CO_2 can interact strongly with the sodium cations (Figure 8).[26–30] Thus, the differences between CO_2 and CH_4 adsorbed amounts into ZA are due mainly to electronic effects.

The structural difference between ZA and ZAS0.3 is that ZA is LTA and ZAS0.3 is CAN. The CAN structure has no sodalite cavities as LTA; instead, it has cancrinite cavities (Table 2). Kowalak et al.[31] have reported the polysulfide occlusion into the CAN structure. Their main conclusion is that the polysulfides are located in CAN cavities but that the resulting materials have less intense coloration compared to the pigments obtained from zeolite A. It can be emphasized that although the cancrinite cavity is smaller than the sodalite cavity, polysulfides may be trapped inside it. Our results are in full agreement with this work and as we obtained the ratio $S_2^-/S_3^- = 0.5$ which determines the color, the shade, and the thermal stability. This sample has a strong blue color which is compared to commercial ultramarine.

We did not find any work reporting adsorption of gases onto sulfur containing zeolites, as most studies are focused on pigment synthesis. However, the solids should present original adsorption properties. If the isotherm of carbon dioxide on ZAS0.3 is compared to ZA, less CO_2 is adsorbed (8.9% less).
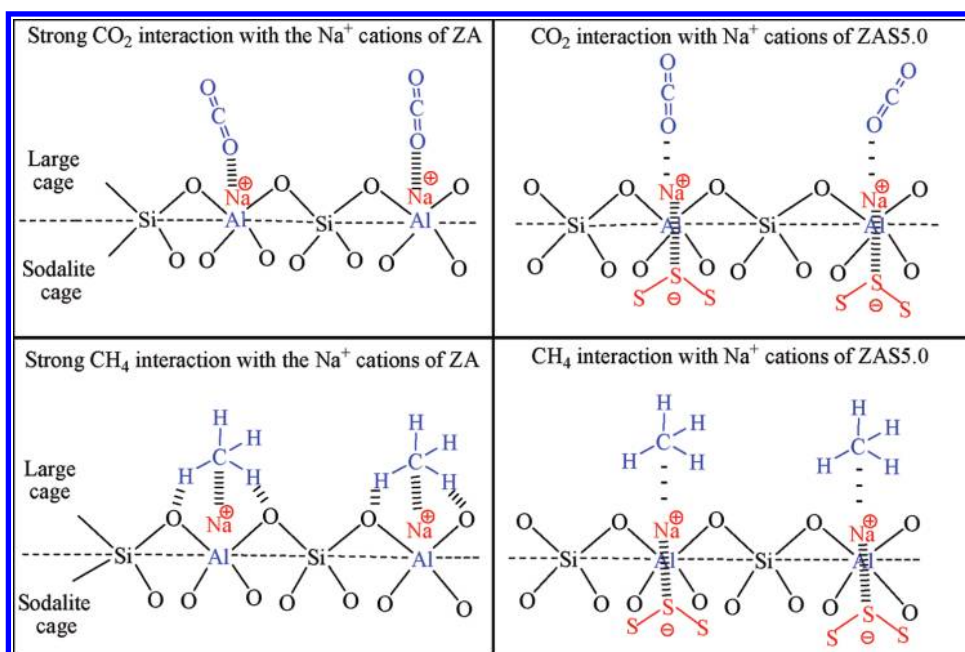

Figure 8. Model to show the interaction between CO_2 or CH_4 in zeolite A and ZAS5.0.
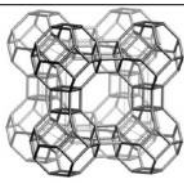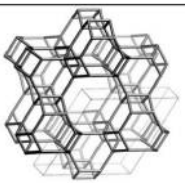
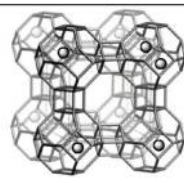**TABLE 2: Structure Details of ZA, ZAS0.3, and ZAS5.0**

TABLE 3: Enthalpies of Adsorption of CO_2 and CH_4 at the Initial Loading

sample	enthalpy (kJ mol^{-1})	
	CO_2	CH_4
ZA	83.56	51.19
ZAS0.3	60.27	30.66
ZAS5.0	39.46	22.41

The window dimension of cancrinite is smaller than that in ZA, and the penetration of gas molecules is more difficult. Still, the large cavity of CAN has a window diameter of 5.9 Å[32] and CO_2 molecules can enter this cavity, but the interaction between negative charges of polysulfides and the positive charge of sodium cations is stronger than the interaction between Na$^+$ and π-electrons of CO_2 molecules. Then, the sodium charge is partially transferred to cancrinite occluded polysulfides. Therefore, the interaction with CO_2 in the large cavity should be very weak, at least weaker than that in ZA.

The ZAS5.0 sample has the same structure as ZA, and the polysulfides are occluded into sodalite cages. The gas molecules can penetrate into the large cavity, but due to the kinetic diameter of CO_2 (3.3 Å) and CH_4 (3.8 Å) they cannot access to sodalite cages. Gas molecules interact by van der Waals forces with the Na$^+$ cation in zeolite A. Polysulfides have a strong effect on the adsorption properties. The charge of Na$^+$ is tuned due to charge transfer to polysulfides. Only 27% of CO_2 was adsorbed even at high pressure (Figure 8).

In both samples ZAS0.3 and ZAS5.0, CH_4 was adsorbed only at very high pressure (higher than 25 bar). Methane molecules do not present a quadrupolar moment or π-electrons as CO_2. Diffusion is, however, more difficult due to molecular size and electronic features, and thus, more pressure is required to reach the same adsorbed amount. However, one should not overlook the fact that the CO_2 and CH_4 experiments were carried out at different reduced temperatures leading to slightly different possibilities of adsorption mechanisms. The amount adsorbed in ZAS0.3 (28.9%) is higher than that in ZAS5.0 (27.8%), as

ZAS0.3 has cancrinite cavities which are smaller than the sodalite cavities of ZAS5.0. The highest polysulfide content samples have less CH_4 amounts adsorbed at 25 bar; we can conclude that the diffusion is controlled by the polysulfide concentration. The adsorbed amount of CH_4 on ZAS5.0 increases slowly with the pressure, whereas on ZAS0.3 it increases faster. At 28 bar, 77% compared with ZA was already adsorbed on ZAS0.3. The interaction between aluminosilicate surface and the methane can associate to van der Waals forces (Figure 8). Methane does not interact with the Na$^+$ cations in the same manner as CO_2.

At low gas loading, ZA interacts strongly with gas molecules and high values of enthalpy were obtained. Indeed, all sodium cations are available to interact with gas molecules. As shown by XRD, in ZAS0.3 and ZAS5.0, chromophores are periodically incorporated in the lattice. Then, a homogeneous adsorption surface was generated and the adsorption enthalpy was constant as pressure increased, confirming this homogeneity within this porous structure. Nevertheless, for low loading, first molecules interact directly with active sites. If we compare the enthalpy values in ZA to ZAS0.3 and ZAS5.0, they are higher; indeed, polysulfides alter the interaction between gas molecules and ZA (Table 3).

Hence, two different hypotheses may be proposed. On the one hand, some Na$^+$ cations can be poisoned by polysulfides and just a small amount of them are not poisoned and they can interact with gas molecules. In such case, enthalpy values have to be similar as those of ZA at initial loading. However, the adsorption enthalpy of ZAS0.3 and ZAS5.0 is smaller than that of ZA. Therefore, this hypothesis has to be discarded. On the other hand, aluminosilicate structure can be electrically modified due to polysulfides and all Na$^+$ charges are altered. Then, interaction between gas molecules and Na$^+$ charge is weak, and thus, enthalpy should be lower than that in the parent structure. In ZAS0.3 and ZAS5.0 samples, the enthalpy is indeed smaller than ZA. Hence, this second proposition is retained.

Na$^+$ Charge Tuning

J. Phys. Chem. C, Vol. 114, No. 17, 2010 **7887**

From UV−vis results, ZAS0.3 has 94.52% of polysulfides and ZAS5.0 only 66.4%, and the interaction between gas molecules and the solid surfaces is due to the polysulfide content and to available Na$^+$ cations in the aluminosilicate structure which is higher in ZAS5.0. We can conclude that the charge of Na$^+$ cations is tuned by S$_3^-$ and S$_2^-$ polysulfides on two different structures (CAN and LTA). Carbon dioxide or methane molecules thus are not able to interact as strongly with Na$^+$ on ZA.

5. Conclusions

We proposed a mechanism of polysulfide occlusion and structural transformation of LTA structure. When S/Na$_2$CO$_3$ is equal to 0.3, the final structure corresponds to hexagonal type cancrinite symmetry and sulfur is incorporated periodically in the network. The mechanism of this synthesis is as follows:

(1) Reaction between sulfur and sodium carbonate to generate polysulfides.
(2) The sodium carbonate in excess reacts with the intracrystalline water around 240 °C, and the structure turns out to be CAN instead of LTA.
(3) Diffusion of polysulfides.
(4) Cooling down has a templating effect and polysulfides are occluded into the cancrinite cavities. The resulting material presents high thermal stability.

At S/Na$_2$CO$_3$ = 5.0, the LTA structure is maintained. The polysulfides S$_2^-$ and S$_3^-$ are occluded into sodalite cages and a three step mechanism is followed:

(1) Reaction between sulfur and sodium carbonate.
(2) Diffusion of polysulfides due to the increasing temperature.
(3) Polysulfide occlusion into sodalite cages.

Methane and carbon dioxide adsorption was used to test the polysulfide effect on the aluminosilicate network. Sodium cations interact with polysulfides, but they cannot interact strongly with gas molecules; the cation charge is then tuned using polysulfides, and the adsorption properties can be tailored.

Supporting Information Available: TGA curve and mass spectrometry data showing the thermal degradation of ZAS5.0. This material is available free of charge via the Internet at http://pubs.acs.org.

References and Notes

(1) Breck, D. W. Zeolites Molecular Sieves. Structure, chemistry, and use Wiley-Interscience Publication: New York, 1974; p 82.
(2) Meier, W. M. *Molecular Sieves*; Soc. Chem. Ind.: London, 1968, p 10.
(3) Matsuoka, S.; Nakamura, H.; Tamura, T. *J. Nucl. Sci. Technol.* **1984**, *21*, 862.
(4) Choi, B. S.; Park, G.; Lee, L. W.; Yang, H. Y.; Ryu, S. K. *J. Radioanal. Nucl. Chem.* **2003**, *256*, 19.
(5) Seel, F. In *Studies in Inorganic Chemistry*; Müller, A., Krebs, B., Eds.; Elsevier Scientific: Amsterdam, The Netherlands, 1984; p 67.
(6) Won Choi, Q.; Choi, H.; Chang, S. Y.; Pyun, C. H.; Kim, C. H. *Bull. Korean Chem. Soc.* **1994**, *15*, 1118.
(7) Gobeltz, N.; Demortier, A.; Leulier, P. J.; Duhayon, C. *J. Chem. Soc., Faraday Trans.* **1998**, *94*, 2257.
(8) Gobeltz, N.; Demortier, A.; Leulier, J. P. *Inorg. Chem.* **1998**, *37*, 136.
(9) Kowalak, S.; Jankowska, A.; Laczkowska, S. *Catal. Today* **2004**, *90*, 167.
(10) Loera, S.; Ibarra, I. A.; Laguna, H.; Lima, E.; Bosch, P.; Lara, V.; Haro-Poniatowski, E. *Ind. Eng. Chem. Res.* **2006**, *45*, 9195.
(11) Llewellyn, P.; Maurin, G. *C. R. Chim.* **2005**, *8* (3−4), 283.
(12) Seff, K. *J. Phys. Chem.* **1972**, *76*, 2601.
(13) Ucum, F. *Z. Naturforsch.* **2002**, *579*, 283.
(14) Stuart, B. *Infrared Spectroscopy: Fundamentals and applications*; Analytical Techniques in Science; John Wiley and Sons: Sussex, England, 2004; p 50.
(15) Clark, R. J. H.; Cobbold, D. G. *Inorg. Chem.* **1978**, *17*, 3169.
(16) Kowalak, S.; Jankowska, A. *Microporous Mesoporous Mater.* **2003**, *61*, 213.
(17) Rouquerol, F.; Rouquerol, J.; Sing, K. Adsorption by powders and porous solids. *Principles, methodology and applications*; Academic Press: London, 1999; p 382.
(18) Gobeltz-Hautecoeur, N.; Demortier, A.; Lede, B.; Lelieur, J. P.; Duhayon, C. *Inorg. Chem.* **2002**, *41*, 2848.
(19) Alvarez, L. J.; Ramirez-Solis, A.; Bosch, P. *Zeolites* **1997**, *18*, 54.
(20) Hund, F. *Z. Anorg. Allg. Chem.* **1984**, *509*, 153.
(21) Subotic, B.; Skritic, D.; Smit, I.; Sekovanic, L. *J. Cryst. Growth* **1980**, *50*, 498.
(22) Subotic, B.; Sekovanic, L. *J. Cryst. Growth* **1986**, *75*, 561.
(23) Barnes, M. C.; Addai-Mensah, J.; Gerson, A. R. *Microporous Mesoporous Mater.* **1999**, *31*, 303.
(24) Deem, M. W.; Newsam, J. M.; Creigthon, J. A. *J. Am. Chem. Soc.* **1992**, *114*, 7198.
(25) Schrimpf, G.; Schlenkirch, M.; Brickmann, J.; Bopp, P. *J. Phys. Chem.* **1992**, *96*, 7404.
(26) Akten, D. E.; Siriwardane, R.; Sholl, S. *Energy Fuels* **2003**, *17*, 977.
(27) Habgood, H. W. *Can. J. Chem.* **1958**, *30*, 1384.
(28) Triebe, R. W.; Tezel, F. H.; Khulbe, K. C. *Gas Sep. Purif.* **1996**, *10*, 81.
(29) Vermesse, J.; Vidal, D.; Malbrunot, P. *Langmuir* **1996**, *12*, 4190.
(30) Triebe, R. W.; Tezel, F. H. *Gas Sep. Purif.* **1995**, *9*, 223.
(31) Kowalak, S.; Jankowska, A.; Zeidler, S. *Microporous Mesoporous Mater.* **2006**, *93*, 111.
(32) Miyake, M.; Akachi, T.; Matsuda, M. *J. Mater. Chem.* **2005**, *15*, 791.